Journal of Basic and Applied Engineering Research
p-ISSN: 2350-0077; e-ISSN: 2350-0255; Volume 3, Issue 5; April-June, 2016, pp. 414-418

http://www.krishisanskriti.org/Publication.html

Effect of Ce Substitution at Mn Site in Magnetic and Transport Properties of $La_{0.7}Ca_{0.3}MnO_3$

Akash Yadav[1], Jyoti Shah[2] and R.K. Kotnala[3]

[1,3]CSIR-National Physical Laboratory, New Delhi 110012, India
[2]DST-Women Scientist, CSIR-NPL, New Delhi 110012, India
E-mail: [1]akashyadav191@rediffmail.com, [2]shah.jyoti1@gmail.com, [3]rkkotnala@nplindia.org

Abstract—*Magnetic and transport properties of $La_{0.7}Ca_{0.3}Mn_{1-x}Ce_xO_3$ (x = 0.0, 0.1, 0.2) compound has been studied. Rietveld analysis of x-ray diffraction pattern confirmed Orthorhombic structure and Pbnm space group along with small amount of unreacted CeO_2. Curie temperature (T_C) was found to decrease from 265 K for x = 0.0 to 250 K for x = 0.2 due to the reduction in long range ferromagnetic ordering. Grain size found to be decreased from 2.5 µm to 0.78 µm with Ce content from x = 0.0 to 0.2 observed by Scanning electron microscopic images. Magnetic moment decreases with increasing Ce substitution in LCMO at 300 K and 80 K. Change in magnetoresistance (MR%) at 20 K was obtained maximum 29.3% for x = 0.1 Ce substitution. Metal insulator transition (MIT) temperature (T_P) shift from 260 K for x = 0.0 to 232 K for x = 0.2 with increasing Ce content was observed by more electron scattering at grain boundary. The induced delocalization of charge carriers with applied magnetic field decreases resistivity, hence MIT shifted to higher temperature. Cerium substitution at Mn site in LCMO results into decrease in double exchange interaction. High MR values observed in the samples confirmed that unreacted CeO_2 could be segregated at grain boundary.*

Keywords*: Magnetoresistance, Grain Size, MIT Temperature, Double Exchange Interaction*

1. INTRODUCTION

The discovery of colossal magnetoresistance (CMR) in mixed valent manganese perovskites, such as $La_{1-x}A_xMnO_3$ (A = Ca, Pb, Sr, and Ba) have high technological and scientific interest due to their spectacular physical properties. CMR materials have versatile field of potential technological applications such as magnetic-field sensor, spintronics materials, memory devices (electroceramics) and magnetocaloric refrigeration [1–6]. The undoped compound $LaMnO_3$ is an antiferromagnetic and showing insulating behaviour at all temperatures and having 143 K Neel temperature [7]. The substitution of diavalent ion such as (Ba, Sr, Pb and Ca) at La site in $LaMnO_3$ as $La_{1-x}A_xMnO_3$, creates Mn^{4+} ions to achieve charge neutrality. In these oxides, the magnetic spins order ferromagnetically, for x = 0.1 to 0.5 near room temperature or below the room temperature. The large negative magnetoresistance observed in $La_{1-x}Sr_xMnO_3$ [8, 9]. Doping effects of transition metal of different radius at Mn site in perovskites $La_{0.7}Ca_{0.3}Mn_{0.95}TM_{0.05}O_3$ (TM = Cr, Fe, Co, Ni, Cu, Zn) investigated and found an interesting correlation between the maximum magnetoresistance, the structure parameters, and the ion radius [10]. Effect on Curie temperature by Ce substitution at La site has been reported to depend on Mn-O-Mn bond angle and Mn-O bond length [11]. There have been no reports of Ce substitution at Mn site in La–Ca–Mn–O system with substantial magnetoresistance effect. The effect on magnetic and transport property in $La_{0.7}Ca_{0.3}Mn_{1-x}Ce_xO_3$ (x = 0.0, 0.1, 0.2) has been investigated. The large negative magnetoresistance (MR%) at low temperature (20 K) was observed for x = 0.1 Ce concentration in this system.

2. EXPERIMENTAL DETAILS

$La_{0.7}Ca_{0.3}Mn_{1-x}Ce_xO_3$ (x = 0.0, 0.1, 0.2) samples were prepared by the conventional solid state reaction method. High-purity precursors La_2O_3, $CaCO_3$, CeO_2 and MnO_2 with appropriate stoichiometric proportions were mixed and ground. The well-mixed oxides and carbonate were then preheated around 1000^0C for 12 h in air. The preheated samples were reground and again heated at 1200^0C for 12 h with intermediate grindings. Finally, obtained calcined samples were pelletized using polyvinyl acetate (PVA) as a binder under a pressure of 6 tons and sintered at 1300^0C for 20 h followed by slow cooling. The crystalline structure of the samples was characterized by X-ray diffractometer (Brukar D-8 Advanced Diffractometer) with CuK_α (λ = 0.154 nm) radiation. The resistivity of the samples have been measured by four-probe method. Temperature-dependent resistivity (ρ-T) measurements were carried out at H = 0 and H = 0.37 Tesla applied magnetic field. Temperature dependent magnetization (M-T) and external magnetic field dependent magnetization (M-H) at 300 K and 80 K of samples were analyzed by vibrating sample magnetometer (Lakeshore-7304). The Grain size and elemental distribution were analyzed by scanning electron microscope (Zeiss EVO MA 10) and energy dispersive X-ray analysis (EDAX) measurements respectively (OXFORD INCA ENERGY 250). The MR% of the samples at 300 K and 20 K were measured by the standard four-probe

method, where a constant current of 1 mA has been applied on the sample from a DC current source (Keithley-6221) in presence of magnetic field varying from 0 – 0.88 Tesla using electromagnet (Bruker). The corresponding voltage drop across the sample was recorded with a nano voltmeter (Keithley-2182A).

3. RESULTS AND DISCUSSIONS

3.1 X-ray Diffraction

The XRD patterns of $La_{0.7}Ca_{0.3}Mn_{1-x}Ce_xO_3$ (x = 0.0, 0.1, 0.2) samples are shown in Fig.1. All the samples were observed in perovskite structure by XRD pattern along with impurity peaks of CeO_2 due to the segregation of CeO_2 at grain boundaries. This was further confirmed by SEM-EDAX measurements. The structural parameters for all samples have been refined by Rietveld fitting of the XRD patterns. Rietveld fitted XRD data for prinstine and x = 0.1 samples are shown in Fig.2. An Orthorhombic structure with Pbnm space group has been observed for all $La_{0.7}Ca_{0.3}Mn_{1-x}Ce_xO_3$ samples. The unit cell parameters and volume was found to be increased with increasing Ce content obtained by rietveld refinement. This increase in unit cell volume with Ce concentration can be attributed to the larger ionic radii of Ce^{4+} ion (~ 0.97 Å) as compared to Mn^{3+} ion (~ 0.64 Å), which results into expansion of unit cell with increasing Ce concentration. The calculated unit cell volume (V) is given in Table.1.

Fig. 1: XRD patterns for $La_{0.7}Ca_{0.3}Mn_{1-x}Ce_xO_3$ (x = 0.0, 0.1, 0.2) series.

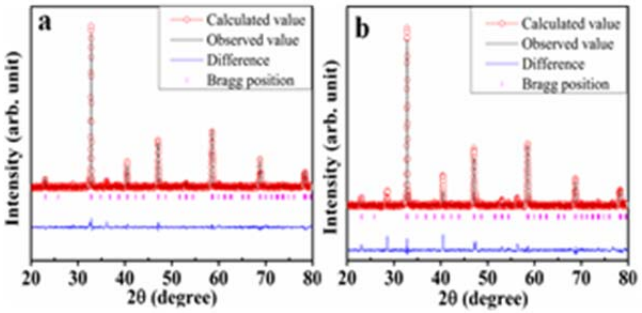

Fig. 2: Rietveld fitted XRD patterns of $La_{0.7}Ca_{0.3}Mn_{1-x}Ce_xO_3$: (a) x = 0.0 and (b) x = 0.10 samples.

3.2 Scanning Electron Microscope (SEM)

SEM images of $La_{0.7}Ca_{0.3}Mn_{1-x}Ce_xO_3$ (x = 0.0 – 0.2) samples are shown in Fig. 3. A continuous decrease in grain size was observed from SEM images with increasing Ce content. EDAX spectra taken at grain and grain boundary were analyzed. It has been determined by EDAX spectra that higher concentration of Ce was present at grain boundary as compared to grains. Concentration of Ce increases at grain boundary with increasing Ce concentration in the prinstine sample and CeO_2 segregated at the grain boundaries, which is also confirmed by extra peaks of CeO_2 in XRD patterns. Cerium oxide presence at grain boundaries creates the insulating grain boundary and impede the grain boundary movement during sintering, thus restricted the grain size. Thus increasing grain boundaries by reduced grain size resulted into drastically increased resistivity due to strong electron scattering at grain boundary regions. This was further confirmed by ρ-T measurements. The average grain size for all the samples are shown in Table 1.

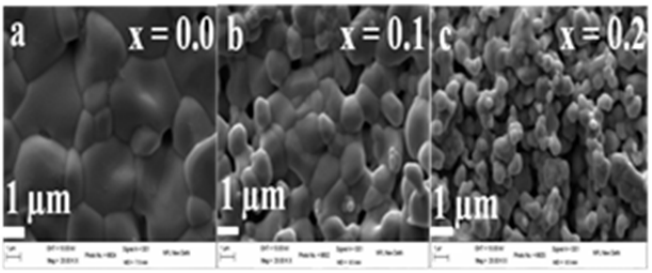

Fig. 3: SEM Images of the Ce substituted $La_{0.7}Ca_{0.3}Mn_{1-x}Ce_xO_3$ ($0 \le x \le 0.2$) samples. (a) for x = 0.0. (b) for x = 0.1. (c) for x = 0.2.

3.3 Electron transport properties

Temperature dependent zero field resistivity measurements for all the samples are hown in Fig.4. The resistivity increased and metal insulator transition temperature (T_P) decreases from 260 K to 232 K with increasing Ce content. It may be due to decreasing grain size and reduction of double exchange interaction. Since Ce does not participate in the double exchange interaction (Mn^{3+} - O - Mn^{4+}). In manganite LCMO the electron conduction depend upon double exchange interaction [12]. Grain boundary also plays an important role in electron conduction mechanism. It has been observed by SEM images that grain boundaries have been increased by Ce substitution. Strong electron scattering from grain boundary region, results into increase in resistivity and reduction in T_P. Broadening of resistivity peak increases with increasing Ce content due to the increasing inhomogenity in the samples [13].

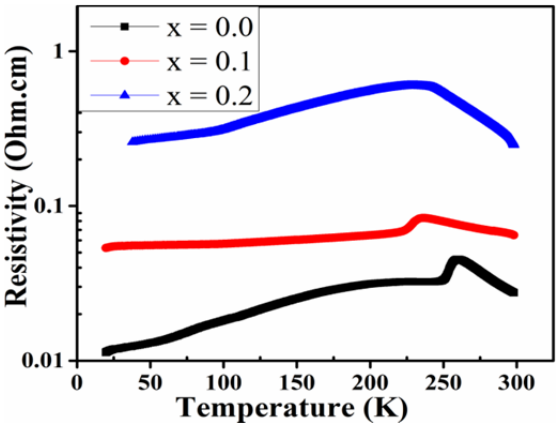

Fig. 4: Temperature dependent resistivity plot for Ce substituted $La_{0.7}Ca_{0.3}Mn_{1-x}Ce_xO_3$ (x = 0.0, 0.1, 0.2) series.

Resistivity versus temperature plot at H = 0 and H = 0.37 Tesla magnetic field for each sample as shown in Fig. 5. These figures clearly show magnetic field has the effect of decrease in resistivity and T_P shifted to higher temperature. It may be due to induces delocalization of charge carriers in $La_{0.7}Ca_{0.3}Mn_{1-x}Ce_xO_3$ (x = 0.0 – 0.2) compound with applied magnetic field, which suppress the resistivity and allow local ordering of the magnetic spins. Due to this ordering, the ferromagnetic metallic (FMM) state may suppress the paramagnetic insulating regime. As a result, the conduction electrons (e^1_g) are completely polarized inside the magnetic domains and are easily transferred between the pairs of Mn^{3+} ($t^3_{2g} e^1$ g : S = 2) and Mn^{4+} ($t^3_{2g} e^o$ g : S = 3/2) via oxygen and hence the resistivity peak temperature (T_P) shifts to high temperature side with applied magnetic field [14-16]. Metal insulator transition temperature (T_P) at H = 0 and H = 0.37 Tesla applied magnetic field are given in Table 1. Shifting of T_P decreases towards higher temperature with applied magnetic field on increasing Ce content is due to the reduction in double exchange interaction. Because Mn^{3+} and Mn^{4+} spins are aligned parallel ~~due to~~ double exchange interaction and electrons easily transfers between Mn ions. Resistivity versus temperature (ρ-T) plots at H = 0 and H = 0.37 T overlaps for x = 0.2 samples, which indicates minimum MR% for this sample due to the porosity developed in the sample as seen in SEM images.

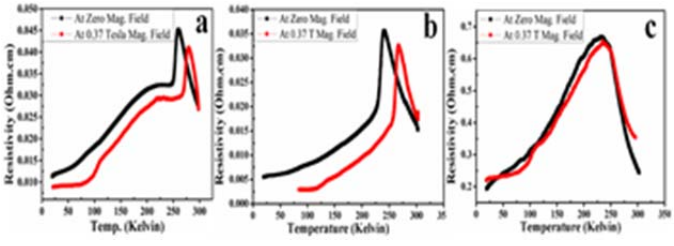

Fig. 5: Resistivity vs. temperature plot at H = 0 and H = 0.37 Tesla magnetic field for Ce substituted $La_{0.7}Ca_{0.3}Mn_{1-x}Ce_xO_3$ (x = 0.0, 0.1, 0.2) series. (a) for x = 0.0. (b) for x = 0.1. (c) for x = 0.2.

1.1. Magnetic properties

1.1.1. M-H measurements

The effect of Ce substitution on magnetization of LCMO samples has been studied at low temperature (80 K) as well as at room temperature (300 K). Magnetization hysteresis (M-H) loops are shown in Fig. 6.

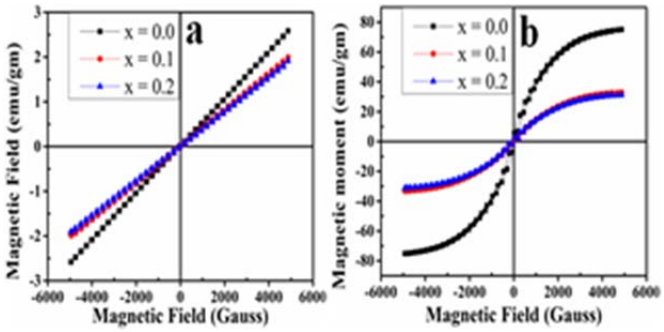

Fig. 6: M-H plot (a) At 300 K and (b) At 80 K Temperature; (a)-(b) for Ce substituted $La_{0.7}Ca_{0.3}Mn_{1-x}Ce_xO_3$ (x = 0.0, 0.1, 0.2) series.

A paramagnetic behavior was observed at room temperature while saturated ferromagnetic behaviour was observed at low temperature (80 K) for all the samples. Room temperature magnetization decreases with increasing Ce content may be due to antiferromagnetic alignments [17]. A reduced value of saturation magnetization (M_S) with increasing Ce concentration at 80 K was observed given in Table.1. The observed low temperature ferromagnetism in these samples is due to Zener double exchange interaction between Mn^{3+}/Mn^{4+} ions [18]. Substitution of Ce at Mn site reduces the double exchange interaction since Ce does not participate in double exchange interaction. The decrease magnetic moment of pure LCMO by x=0.1 Ce is ~ 42 emu/g while only ~ 1 emu/g decrease in M_S observed for x = 0.2 Ce concentration. It may be due to limited solubility of Ce inside LCMO lattice. Beyond the solubility limit, CeO2 segregates at grain boundary as also confirmed by EDAX spectra. Hence on further increasing Ce content magnetic moment is not varying significantly.

3.4.2. M-T measurements

Fig.7. shows magnetization vs. temperature (M-T) plot for all Ce substituted $L_{0.7}Ca_{0.3}Mn_{1-x}Ce_xO_3$ samples at 1 kOe applied magnetic field. A continuous decrease in Curie temperature with increase in Ce concentration was clearly observed from inset of Fig.7.

The observed decrease in Curie temperature can be ascribed to the reduced long range ferromagnetic ordering with increasing Ce concentration. Long range ferromagnetic ordering in LCMO sample arises due to double exchange interaction between Mn^{3+} and Mn^{4+} ions. Increasing Ce concentration led to reduced long range ferromagnetic ordering. It was also observed that resistivity peak appeared at a temperature much

lower than the Curie temperature which confirms local magnetic disorder or inhomogeneities arising from atomic short-range order due to Ce substitution [17, 19]. Curie temperature for all the samples given in Table.1.

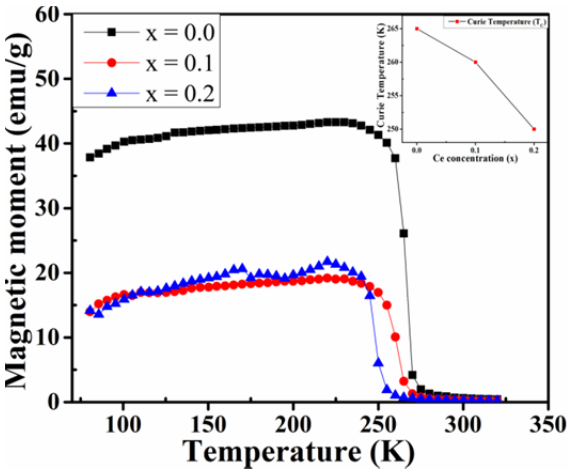

Fig. 7: Magnetic moment vs. temperature for $La_{0.7}Ca_{0.3}Mn_{1-x}Ce_xO_3$ (x = 0.0, 0.1, 0.2) at an applied field of 1000 Oe, with inset of Curie temperature (T_C) vs. Ce concentration (x).

3.5 Magnetoresistance measurements

Fig.8. represents variation in MR% with increasing Ce concentration for low temperature (20 K) as well as room temperature (300 K).

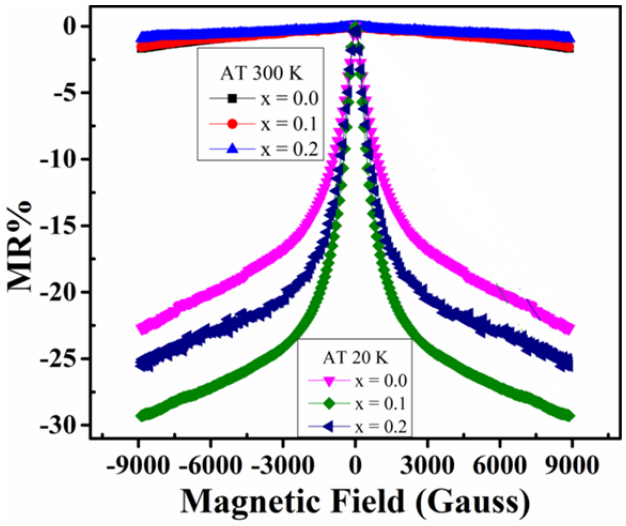

Fig. 8: Field dependence MR% at 300 K and 20 K.

Room temperature MR% was found to be systematically reduced with increasing Ce concentration from -1.65% for x = 0.0 to -0.93% for x = 0.2. This kind of behaviour can be explained by magnetic polaron formation above ferromagnetic ordering temperature (T_c). It has been observed that conduction in paramagnetic phase of rare earth manganites is due to small polaron hopping [20]. Local lattice distortions led to localization of e_g electron which polarizes the spin of neighboring ions resulting into polaron formation above T_c [21]. Applied magnetic field delocalizes the e_g electron which results into large change in resistivity. In pure LCMO sample MIT (T_P) was observed in the vicinity of Curie temperature (T_c) from (M–T) and (ρ–T) plots which close to room temperature. Magnetic polaron formation results in large magnetoresistance at room temperature which is contiguous to Curie temperature. However, Ce substitution results into shift of T_c from MIT (T_P) and the difference increases with increasing Ce concentration. This led to smaller change in resistance with applied magnetic field in Ce substituted LCMO samples due to less contribution from small polaron hopping. A significant effect of Ce content was observed at low temperature (20 K) MR, which shows a large change in MR%. First the magnetoresistance was found to be increased maximum up to ~ 29.3% for x = 0.10 concentration after which it reduced. Because CeO_2 segregates at grain boundary region and creates insulating grain boundaries and decreases grain size with increasing Ce content, which results into strong scattering of electrons from grain boundary region, it reveals increasing resistivity and increasing low temperature MR%. It has been already confirmed by resistivity measurements. After x = 0.10 concentrations porosity increases that reduces electron transfer channel between the grains resulted in very strong scattering of electrons. Hence a drastically increasing resistivity and decreasing MR% observed for x=0.2 sample.

Table 1: Parameters from magnetoresistance, transport and magnetic properties of Ce substituted $La_{0.7}Ca_{0.3}Mn_{1-x}Ce_xO3$ (x = 0.0, 0.1, 0.2) series.

Ce Content (x)	MR% At 20 K	Tp at Zero M.F (K)	Tp at 0.37 T M.F (K)	Tc (K)	MS at 80 K (emu/g)	V (A0)3	Grain Size (μm)
0.0	-22.71	260.6	266.3	265	75.04	229.7	2.5
0.1	-29.29	242	246.6	260	32.8	229.9	1.3
0.2	-25.54	232	235.2	250	31.2	230.2	0.79

4. CONCLUSION

In summary, effects of Ce substitution on magnetotransport and magnetization properties of $La_{0.7}Ca_{0.3}Mn_{1-x}Ce_xO_3$ (x = 0.0, 0.1, 0.2) samples have been investigated. Almost single phase formation of Ce substituted LCMO was confirmed by XRD analysis along with small amount of CeO_2. The increase in the unit cell volume may be due to the larger ionic radii of Ce^{4+} ion (~ 0.97 Å) as compared to Mn^{3+} ion (~ 0.64Å). Grain size decreased with increasing Ce content and unreacted CeO_2 segregates at grain boundary. A large increase in resistivity and decrease in T_P was observed with increase in Ce concentration. Paramagnetic behaviour at room temperature and ferromagnetic behaviour at low temperature (80 K) have been observed in all samples. Decreased T_C with increasing Ce content obtained due to the reduction of double exchange interaction. A drastic increase in magnetoresistance ~ 29%

was observed at x = 0.10 concentration of Ce at low temperature (20 K) as compared to pure LCMO sample. We can say that very small amount of Ce substitution in $La_{0.7}Ca_{0.3}Mn_{1-x}Ce_xO_3$ system controlled the magnetic and transport property (double exchange interaction).

5. ACKNOWLEDGEMENTS

The authors are grateful to the Director "National Physical Laboratory" New Delhi for providing constant encouragement, motivation and support to carry out this work and CSIR-UGC, India for providing financial assistance to carry out the research activity.

REFERENCES

[1] Jin, S. M. Mc Cormack, T. Tiefel, R. Ramesh "Colossal magnetoresistance in La-Ca-Mn-O ferromagnetic thin films." *Journal of Applied Physics* 76.10 (1994): 6929-6933.

[2] L. Balcells, R. Enrich, J. Mora, A. Calleja, J. Fontcuberta, X. Obradors, Manganese perovskites: Thick-film based position sensors fabrication, *Applied physics letters,* 69 (1996) 1486-1488.

[3] A. Lussier, J. Dvorak, S. Stadler, J. Holroyd, M. Liberati, E. Arenholz, S. Ogale, T. Wu, T. Venkatesan, Y. Idzerda, Stress relaxation of $La_{1/2}Sr_{1/2}MnO_3$ and $La_{2/3}Ca_{1/3}MnO_3$ at solid oxide fuel cell interfaces, *Thin Solid Films,* 516 (2008) 880-884.

[4] K. Miyazaki, N. Sugimura, K. Matsuoka, Y. Iriyama, T. Abe, M. Matsuoka, Z. Ogumi, Perovskite-type oxides $La_{1-x}Sr_x MnO_3$ for cathode catalysts in direct ethylene glycol alkaline fuel cells, *Journal of Power Sources,* 178 (2008) 683-686.

[5] A. Lisauskas, S. Khartsev, A. Grishin, Tailoring the colossal magnetoresistivity: $La_{0.7}(Pb_{0.63}Sr_{0.37})_{0.3}MnO_3$ thin-film uncooled bolometer, *Applied physics letters,* 77 (2000) 756-758.

[6] M.-H. Phan, H.-X. Peng, S.-C. Yu, N.D. Tho, H.N. Nhat, N. Chau, Manganese perovskites for room temperature magnetic refrigeration applications, *Journal of magnetism and magnetic materials,* 316 (2007) e562-e565.

[7] A. Urushibara, Y. Moritomo, T. Arima, A. Asamitsu, G. Kido, Y. Tokura, Insulator-metal transition and giant magnetoresistance in $La_{1-x}Sr_xMnO_3$, *Physical Review B,* 51 (1995) 14103.

[8] C. Zener, Interaction between the d-shells in the transition metals. II. Ferromagnetic compounds of manganese with perovskite structure, *Physical Review,* 82 (1951) 403.

[9] A. Millis, B.I. Shraiman, R. Mueller, Dynamic Jahn-Teller effect and colossal magnetoresistance in $La_{1-x}Sr_xMnO_3$, *Physical review letters,* 77 (1996) 175.

[10] K. Ghosh, S. Ogale, R. Ramesh, R. Greene, T. Venkatesan, K. Gapchup, R. Bathe, S. Patil, Transition-element doping effects in $La_{0.7}Ca_{0.3}MnO_3$, *Physical Review B,* 59 (1999) 533.

[11] S. Othmani, M. Bejar, A. Tozri, E. Dhari, E. Hlil, The Effect of Electron Doping on the Physical Properties of $La_{1-x}Ce_xMnO_3$ Manganites, *Ferroelectrics,* 371 (2008) 119-126.

[12] J. Gulley, V. Jaccarino, Impure Exchange-Coupled Paramagnets; Electron-Paramagnetic-Resonance Studies, *Physical Review B,* 6 (1972) 58.

[13] D. Das, C. Srivastava, D. Bahadur, A. Nigam, S. Malik, Magnetic and electrical transport properties of $La_{0.67}Ca_{0.33}MnO_3$ (LCMO): xZnO composites, *Journal of Physics: Condensed Matter,* 16 (2004) 4089.

[14] A. Banerjee, S. Pal, B. Chaudhuri, Nature of small-polaron hopping conduction and the effect of Cr doping on the transport properties of rare-earth manganite $La_{0.5}Pb_{0.5}Mn_{1-x}Cr_xO_3$, *Journal of Chemical Physics,* 115 (2001) 1550-1558.

[15] X. Cao, J. Fang, K. Li, Electrical transport properties in magnetoresistive $La_{0.67}Ca_{0.33}MnO_3$ thin film, *Solid state communications,* 115 (2000) 201-205.

[16] G. Venkataiah, Y. Lakshmi, P.V. Reddy, Influence of sintering temperature on resistivity, magnetoresistance and thermopower of $La_{0.67}Ca_{0.33}MnO_3$, *PMC Physics B,* 1 (2008) 7.

[17] M. Gupta, R. Kotnala, W. Khan, A. Azam, A. Naqvi, Magnetic, transport and magnetoresistance behavior of Ni doped $La_{0.67}Sr_{0.33}Mn_{1-x}Ni_xO_3$ ($0.00 \leq x \leq 0.09$) system, *Journal of Solid State Chemistry,* 204 (2013) 205-212.

[18] C. Zener, Interaction between the d shells in the transition metals, *Physical Review,* 81 (1951) 440.

[19] S. Ogale, R. Shreekala, R. Bathe, S. Date, S. Patil, B. Hannoyer, F. Petit, G. Marest, Transport properties, magnetic ordering, and hyperfine interactions in Fe-doped $La_{0.75}Ca_{0.25}MnO_3$: Localization-delocalization transition, *Physical Review B,* 57 (1998) 7841.

[20] S. Sagar, M. Anantharaman, On conduction mechanism in paramagnetic phase of Gd based manganites, *Bulletin of Materials Science,* 35 (2012) 41-45.

[21] J. Liu, I. Chang, S. Irons, P. Klavins, R. Shelton, K. Song, S. Wasserman, Giant magnetoresistance at 300 K in single crystals of $La_{0.65}(PbCa)_{0.35}MnO_3$, *Applied physics letters,* 66 (1995) 3218-3220.